

I.V. Vakaliuk, R.S. Yavorskyi, L.I. Nykyruy, B.P. Naidych, Ya.S. Yavorskyi

Morphology and optical properties of CdS thin films prepared by Physical Vapor Deposition method

Vasyl Stefanyk Precarpathian National University, Ivano-Frankivsk, Ukraine, r.yavorskyi@pnu.edu.ua

The optical properties of cadmium sulfide thin films obtained by thermal evaporation in vacuum were studied. The stoichiometric compositions of the binary compound previously synthesized from high-purity powders of the initial components were used. Films of different thicknesses deposited on a glass substrate were investigated using scanning electron microscopy and absorption coefficient was defined by the Swanepoel method. It was found that with increasing film thickness, surface formations decrease and at a thickness of 1 μm the film surface is continuous. It is determined that thin films of cadmium sulfide have optimal optical parameters for use as photovoltaic buffer layer. All the obtained films except the film with a thickness of 1215 nm show the usual interference pattern in the reflection spectra.

Keywords: CdS, PVD, absorption coefficient, optical transmission spectra, optical reflection spectra, optical bandgap.

Received 16 November 2021; Accepted 30 November 2022.

Introduction

Cadmium sulfide (CdS) belongs to the II–VI semiconductor compounds, continues to be the subject of intense research due to its wide direct optical bandgap and stability [1]. CdS is an important semiconductor material used in various applications in electro-optic, infrared devices, and as an interlayer in solar cells as well as cadmium telluride (CdTe), copper indium selenide (CIS), copper indium gallium selenide (CIGS), and more recently investigated copper-zinc-tin sulfide (CZTS), and $\text{TiO}_2/\text{Cu}_2\text{O}$ [2-3].

Bulk CdS is a non-stoichiometric n-type semiconductor with a direct bandgap of 2.42 eV. The bandgap of CdS is in the visible region of the electromagnetic spectrum and it leads to the high photosensitivity of CdS in this spectrum [4]. Depending on the choice of synthesis method and annealing temperature, CdS crystallizes in two modifications: cubic sphalerite and hexagonal wurtzite lattice type [5].

Cadmium sulfide is actively used as a thin n-type window layer in CdTe thin film solar cells [6-7]. The main function of the window layer of a thin-film solar cell is the

formation of a junction with the absorber layer while allowing the greatest amount of light to pass through the transition region and the absorber layer. In CdTe solar cells, the correct material selection and optimization of the window layer are important, as it plays an essential role in the transmission of light to the absorber layer. A wide-bandgap semiconductor with a thickness in range of 50–100 nm is used in the cell structure as a window layer to achieve high optical bandwidth and minimal resistive losses [8]. CdS has received a lot of attention due to its perspective optoelectronic properties. The authors [9] established optical studies of CdS thin films and it was found that the transmittance exceeds 80 %. This confirms the ability of the CdS layer to transmit light that enters the p-type absorber layer in the heterojunction solar cell. The optical transparency of the film can be easily controlled by changing its thickness. The CdS layer plays a key role in creating heterojunctions in solar cell structures. Among all heterojunction solar cells, such as CdTe, CIGS, and CZTS, CdS is one of the best candidates as an n-type buffer layer because it facilitates smaller interface defects and exhibits good lattice matching properties. CdS has n-type of conductivity due to the presence of internal donor

defects, i.e., S-vacancies and Cd interstitials in the films. Due to higher miscibility with "neighbors" in the heterostructure, it is included as a sandwich layer between absorber and transparent conductive oxide (TCO) layer in solar cell devices [10]. Favorable crystal symmetry, high optical transparency, appropriate bandgap, superior thermal and chemical stability, and easy doping process (it can reach over 10^{19} cm^{-3}) provide numerous optoelectronic properties of CdS thin films that are extremely useful in optoelectronic devices, as well as solar cells. Besides, the inclusion of a thin CdS layer is crucial for that devices, as a thin CdS layer compared to its thick counterpart allows for a more efficient transfer of the blue region of the light spectrum into the active layer, which ultimately increases the short-circuit current density.

Various chemical and physical methods are used to deposit CdS thin films, for example, thermal evaporation [11, 12], chemical bath deposition (CBD) [13-15], pulsed direct current magnetron sputtering [16], electrochemical atomic layer deposition [17], hot wall deposition method [18], chemical surface deposition [19], screen printing [20], molecular beam epitaxy (MBE) [21[21]] etc. In all these methods, much effort has been devoted to obtaining high-quality CdS thin film by optimizing various parameters such as deposition time and substrate temperature. The results show that the physical properties and crystalline qualities of CdS films strongly depend on the deposition parameters.

I. Experiment

The synthesis of cadmium sulfide was carried out in quartz ampules by fusing elements of cadmium (KD0000) and sulfur (TV-4) (according to the certificate, the content of the main substance is not less than 99.999% and 99.997%, respectively) taken in stoichiometric ratios, with an accuracy of 10^{-4} g. Before, the elements were additionally refined by zone melting method. The concentration of background impurities in the initial components did not exceed 10^{-5} wt. %. The obtained CdS

samples were periodically checked for the content of uncontrolled impurities by laser mass spectrometry methods. CdS thin films were obtained by vacuum thermal evaporation of pre-synthesized Cd-S compounds. Previously chemically cleaned glass plates were used as substrates. The evaporator temperature was $T_E = 880 \text{ }^\circ\text{C}$, the substrate temperature was $T_S = 200 \text{ }^\circ\text{C}$, and the deposition time $\tau = (60\text{--}150)$ sec, as indicated in Table I.

The thicknesses of samples were analyzed by Bruker Dektak XT profilometer. Optical transmission and reflectance spectra investigated using measuring transmittance T and R at normal incidence and room temperature. The measurements were carried out in the wavelength range of (180 – 3300) nm with 1 nm step using Agilent Technologies Cary Series UV-Vis-NIR Spectrophotometer.

II. Results and discussion

The EDS spectrum for samples 1b, 2b and 3a of different thicknesses is presented in Fig. 1. It was established that the deposited films are characterized by a stoichiometric composition, regardless of the film thickness. In particular, the data of phase analysis on glass substrates is shown in Table II and the percentages of atomic mass are Cd ~ 55% and S ~ 43%.

The morphology of CdS thin films was studied using scanning electron microscopy data. The technological parameters of films for research are given in Table I. Films were deposited on glass substrates. For analysis, it is convenient to fix certain technological modes while changing others. In this way, the obtained data were generalized and conclusions were drawn.

The SEM images of the films and the images are shown on Fig. 2 – 4 and are ordered of the increasing thickness of the samples, which was determined by the deposition time.

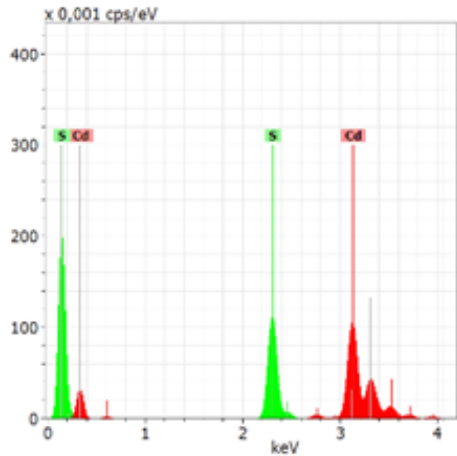
Table I

The technological parameters for obtaining CdS thin films deposited on a glass substrate.

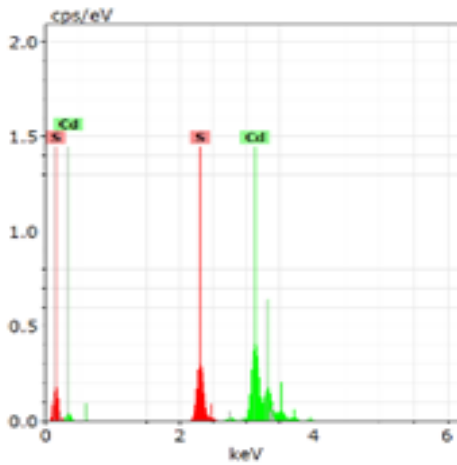
Sample No	Substrate temperature, T_S °C	Evaporation temperature T_E , °C	Deposition time τ , sec	Thickness d, nm
1a	200	880	90	560
1b	200	880	90	560
2a	200	880	60	420
2b	200	880	60	420
3a	200	880	90	540
3b	200	880	90	540
4a	200	880	90	515
4b	200	880	90	515
5a	200	880	150	1215
5b	200	880	150	1215

Phase analysis data for CdS thin films / glass (sample 3a).

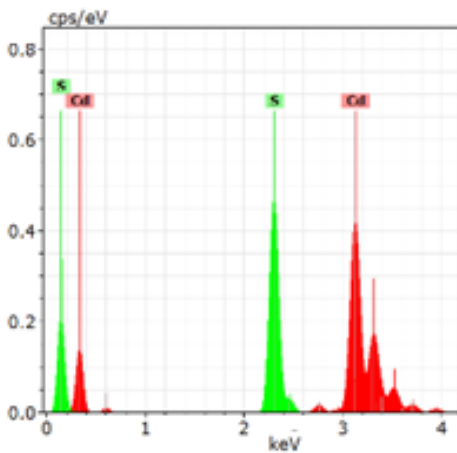
Element	Atomic number	Series	Net	wt. %	[norm. wt. %]	[norm. at. %]	Error in wt. % (3 Sigma)
Cadmium	48	L-series	5222	38.70988	81.72197	56.05184	81.72197
Sulfur	16	K-series	3333	8.657898	18.27803	43.94816	18.27803
			Sum:	47.36778	100	100	



a)

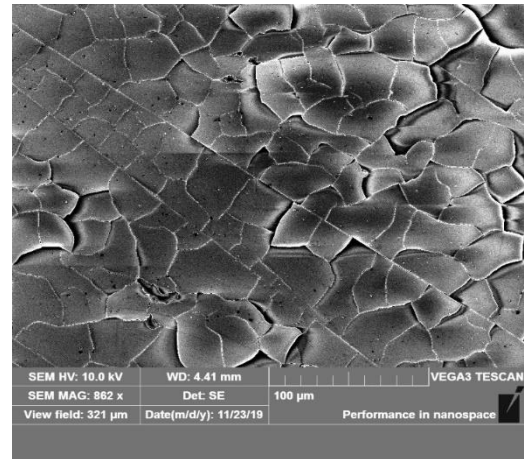


b)

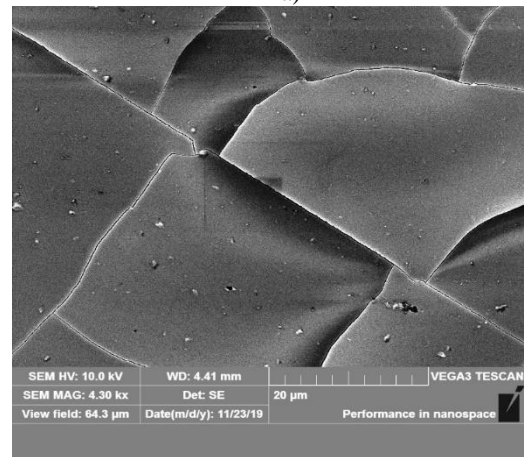


c)

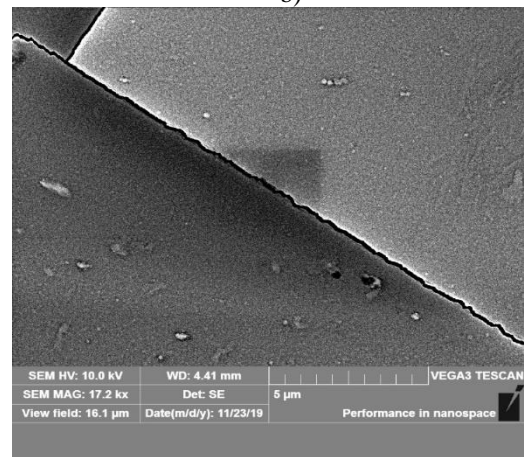
Fig. 1. EDS- spectra of CdS/glass thin films: a) sample 1a, b) sample 2b, c) sample 3a.



a)

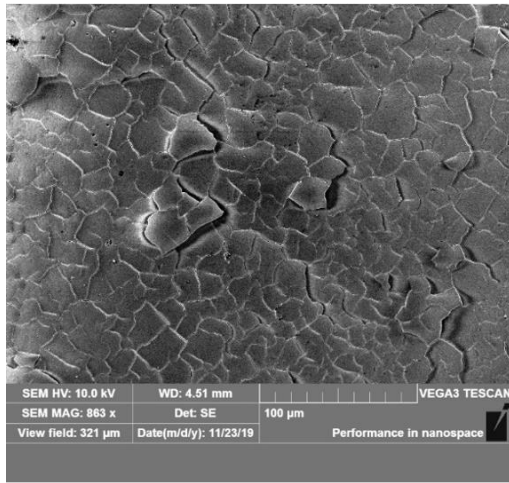


b)

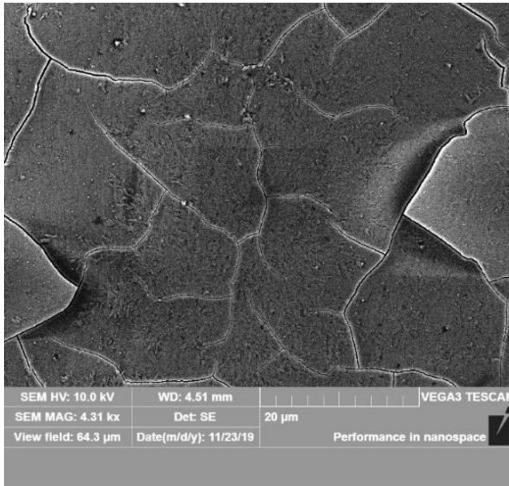


c)

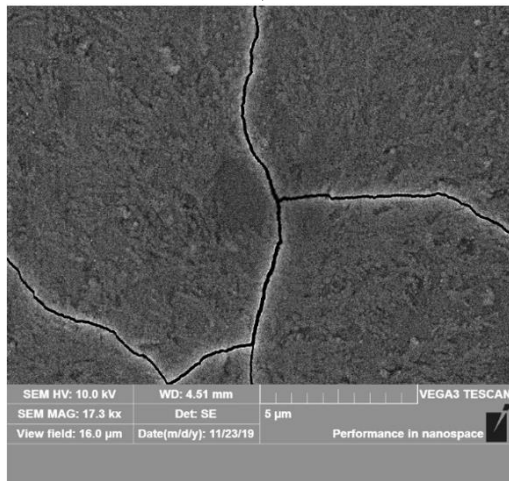
Fig. 2. CdS 2b. Substrate temperature $T_S = 200^\circ\text{C}$, temperature of evaporation $T_E = 880^\circ\text{C}$, deposition time $\tau = 60$ sec, film thickness $d = 420$ nm.



a)



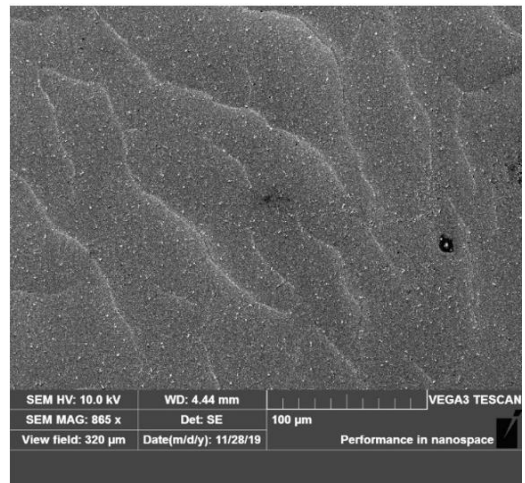
b)



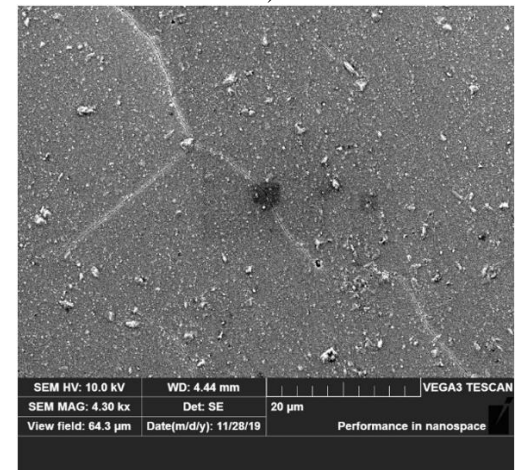
c)

Fig. 3. CdS 1b. Substrate temperature $T_S = 200^\circ\text{C}$, temperature of evaporation $T_E = 880^\circ\text{C}$, deposition time $\tau = 90$ sec, film thickness $d = 560$ nm.

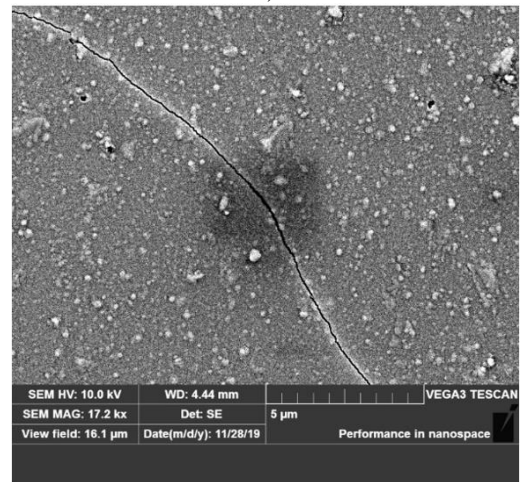
As can be seen, the surfaces of films of smaller thicknesses have a "scale" structure, that is, the condensate forms individual plates on the surface of the film. The size of these plates and their very presence is determined by the time of deposition. In particular, summarizing the data from Fig. 2, b and Fig. 3, b, it can be concluded that an increase in the deposition time leads to a decrease in the lateral dimensions of the "scales": from about $30 \mu\text{m}$ at a



a)



b)



c)

Fig. 4. CdS 3a. Substrate temperature $T_S = 200^\circ\text{C}$, temperature of evaporation $T_E = 880^\circ\text{C}$, deposition time $\tau = 90$ sec, film thickness $d = 540$ nm.

deposition time of 60 sec to $\sim 20 \mu\text{m}$ at a deposition time of 90 sec.

Assuming that the surface plates decrease in size, it can be suggested that the process of their fusion begins as the deposition time increases. A further increase in the deposition time leads to a blurring of the outlines of such plates, and for the thickest films, it is completely absent. In favor of this hypothesis, the fact that for small film thicknesses the combination of such plates into certain

complexes, which are shown in Fig. 2, and Fig. 3, a. The sizes and number of such plate complexes also decrease with the films thickness. If for the thinnest films it is possible to observe complexes of plates with linear dimensions of 50-100 microns, which include several plates of "scales", then for thicker ones, the dimensions first become about 30 microns (Fig. 3, a, 2-3 plates of "scales" are included), and then they disappear altogether (Fig. 4).

The explanation for such processes may be that the heater temperature was chosen relatively high. Under such conditions, the process of condensate deposition will be carried out at higher speeds, and the films will be formed in rather non-equilibrium conditions, which contributes to greater resistance and better properties for applications in photovoltaics. At the same time, internal stresses arise at the "substrate-melt" interface [22-24] and the formation of separate "scale" plates begins, which corresponds to deposition according to the Stransky-Krastanov mechanism (layer-by-layer growth of condensate).

Accordingly, we can draw a general conclusion that as the deposition time increases, the surface plates become smaller and, starting from thicknesses higher than 1000 nm, the plates are not identified as separate flat objects and can be considered as a continuous surface (the array of plates turns into an array individual points and further — on a continuous surface). For such films, which are characterized by a continuous surface, its analysis is made in the corresponding section on the study of AFM data. The absence of such plates is clearly visible on the enlarged image of a thicker film.

III. Optical properties

The study of optical properties such as bandgap, transmission, reflection and refractive index are of great importance for applications in optoelectronics [25]. Thin CdS films of different thicknesses deposited on glass substrates were used for the study. The technological parameters of the deposited films are shown in Table I. The optical properties of CdS thin films were studied as a function of transmittance versus wavelength. The transmission coefficient depends on the structure of the film, which is determined by the production method, deposition conditions, and film thickness. Can be observed the periodic peaks and troughs due to interference phenomena, which indicates the high structural perfection of the thin films. In the case of an imperfect surface, the interference pattern was not observed due to significant scattering and diffuse reflection [26].

The transmission spectra of CdS thin films of different thicknesses obtained on glass substrates were measured in the wavelength range from 180 to 3500 nm and presented in fig. 5. A strong absorption edge at ~500 nm is observed in CdS thin films obtained by open evaporation in vacuum. It can be seen that the films have high transmittance in the visible and near-infrared regions of the spectrum of about 70–95%. The high transmittance value is suitable for solar cell applications where CdS can be used as a window material in heterojunction solar cells such as CdS/CdTe. For a film with a thickness of 1215 nm,

the transmittance increases with increasing wavelength in the entire range, while for films with a thickness of 420 nm, 515 nm, 520 nm, 560 nm, there is a rise and fall in the transmittance. It is considered that such changes are caused by the interference of light passing through the thin film and the substrate [27].

The value of the optical bandgap of the deposited CdS thin films was calculated from the data of the absorption spectra using Tauc's ratio [28]:

$$\alpha = \frac{1}{d} \ln\left(\frac{1}{T}\right), \quad (1)$$

where T and d represent the percent transmittance and film thickness, respectively. The relationship between the absorption coefficient (α) and the optical bandgap (E_g) film can be expressed by the following equation

$$(\alpha h\nu)^2 = A(h\nu - E_g), \quad (2)$$

where A is a constant that depends on the nature of the transition occurring in the films, h is Planck's constant, and ν is the frequency of the photon of the illuminated radiation, E_g is the bandgap width.

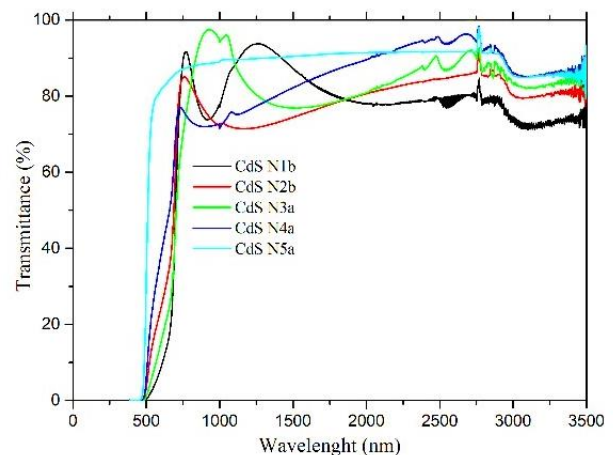


Fig. 5. Optical transmission spectra of CdS/glass thin films of different thicknesses.

As shown in Fig. 6, the optical absorption approaches zero at lower photon energies, but not to absolute zero. This phenomenon is usually called the Urbach tail effect [29-31]. The change in the energy gap of bilayer films can be a consequence of improved morphology or reduced number of defects. Defects create an absorption tail in the absorption spectrum, which further extends into the forbidden zone [32]. This absorption tail is called the Urbach tail and is associated with the Urbach energy. The Urbach energy is also associated with localized states of the amorphous structure in amorphous materials. Polycrystalline materials also have Urbach energy in the band gap due to the presence of disordered atoms in the amorphous phase. Expansion of energy bands reduces the optical bandwidth in materials [33]. Usually, the Urbach energy indicates the disorder of phonon states in the film. The Urbach energy is determined by structural disorder, imperfect stoichiometry and passivation on the surface [34]. The optical bandgap (E_g) of all CdS thin films is calculated by plotting the square of the absorption

coefficient times the photon energy from the incident photon energy (Fig.6), known as a "Tauc" plot [[35]]. At the bandgap energy, the generation of the absorption edge due to electron-phonon interaction or exciton-phonon interaction near the bandgap, CdS films show linearity of the square of the exponent, which is a sign of strong absorption, while the absorption saturates at higher photon energies and the curve deviates from its linearity [29, 30]. E_g is estimated by extrapolating the linear part $(\alpha h\nu)^2$ onto the x-axis.

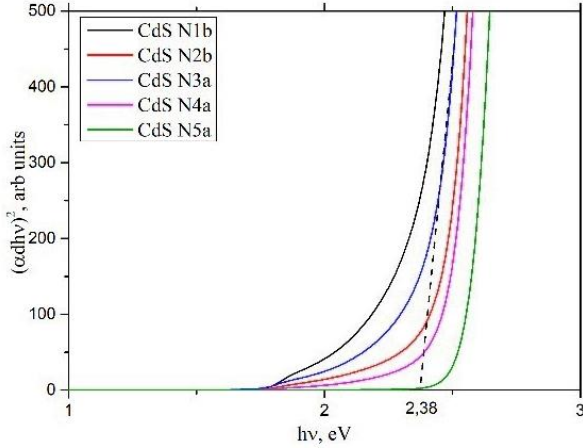


Fig. 6. Optical bandgap of CdS thin films of different thicknesses.

In Fig.6. five graphs of the dependence of $(\alpha h\nu)^2$ on $h\nu$ obtained by the Tauc formula [36] are shown. The direct forbidden zone is estimated by extrapolation from the intersection of the linear part at $\alpha = 0$. The spectral dependence of absorption for CdS films on the Tauc plot shows the presence of a fundamental absorption limit ($E_g = 2.38$ eV). The linear nature of the dependences $(\alpha h\nu)^2 = f(h\nu)$ indicates the formation of the absorption edge by direct interband optical transitions. The obtained optical bandgap values are in good agreement with the standard bandgap values, which are in the range of 2.28–2.46 eV [37-39].

The experimentally established dependence of the reflection coefficient of CdS/glass films of different thicknesses is shown on the Fig.7. With the exception of the film with a thickness of 1215 nm, all other films show the usual interference pattern in the reflection spectra.

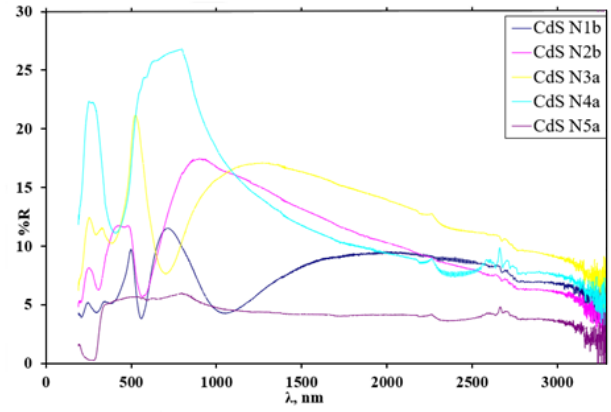


Fig. 7. The optical reflection spectra of CdS/glass thin films of different thicknesses.

One of the most popular methods that uses these interference bands to determine the optical properties of a material is the Swanepoel method [40, 41], which uses interference fringes. It is possible to determine the optical constants of the film, such as refractive index (n), film thickness (d), absorption coefficient (α) and optical conductivity (σ_{opt}). The application of this method is based on the calculation of the maximum $T_m(\lambda)$ and minimum $T_m(\lambda)$ of the transmission curve by parabolic interpolation to the experimentally determined positions of the maxima and minima. Similar calculations were carried out by the authors [42-44] for CdTe thin films, which shows the effect of the deposition technology on the morphology and optical properties of cadmium telluride thin films, as well as on the growth processes of thin films.

The refractive index is determined by:

$$n = [N + (N^2 - s^2)^{1/2}]^{1/2}, \quad (3)$$

where

$$N = \frac{2s(T_M - T_m)}{T_M T_m} + \frac{(s^2 + 1)}{2}. \quad (4)$$

Using equations (1) and (2), taking into account the substrate index $s = 0.94$, the refractive index of CdS samples can be obtained. The calculated values of the refractive index (n) are presented in Table III.

The film thickness can be calculated using equation:

$$d = \frac{\lambda_1 \lambda_2}{2(\lambda_1 n(\lambda_2) - \lambda_2 n(\lambda_1))}, \quad (5)$$

Table III

Optical parameters (experimental) and calculated results of CdS sample 1b thin film.

λ , nm	T_{max}	T_{min}	n	d_1 , nm	m	α , 10^4 cm^{-1}	σ_{opt} , 10^{14}
771	91.71	73.3	1.437358				
914	92.68	73.75	1.437475				
1257	93.79	74.77	1.437257	693.602	2	4.7	1.62033
2158	88.33	77.8	1.432744	550.172	1	5.9	2.03796
				$\langle d \rangle = d = 621.887$			

where $n(\lambda_1)$ and $n(\lambda_2)$ – refractive index at two adjacent maxima or minima at λ_1 i λ_2 respectively.

For the CdS sample No. 1b, the calculated values of the film thickness are presented in the table as d_1 . The measured experimental thickness value was obtained by the profilometer method (Table I) and is 560 nm. Comparing the experimental data and calculated thickness values, it can be noted that they are in good agreement, and a small difference is due to the error of experimental studies.

Interference order:

$$m = \left[\frac{\lambda_2}{\lambda_1 - \lambda_2} \right], \quad (6)$$

where λ_1 i λ_2 – wavelengths of two adjacent maxima of the interference pattern.

Knowing the following values of the thickness (d) of the thin films deposited on a glass substrate, the refractive index of the sample (n) and the refractive index of the substrate (s), the absorption coefficient of the material can be calculated (α):

$$\alpha = \frac{1}{d} \ln \frac{(n-1)^3(n-s)^3}{E_m - [E_m^2 - (n^2-1)^3(n^3-s^4)]^{1/2}}, \quad (7)$$

where

$$E_m = (8n^2s/T_m) - (n^2 - 1)(n^2 - s^2). \quad (8)$$

Using the obtained values of the absorption coefficient by the Swanepoel method, we can analyze the value of optical conductivity σ_{opt} . The optical conductivity values for sample No. 1b are given in Table III.

The optical conductivity of different thicknesses of CdS is calculated by the equation:

$$\sigma_{opt} = \frac{\alpha n c}{4\pi} \quad (9)$$

where α – is the absorption coefficient, and c is the speed of light.

Conclusions

The surface plates become smaller as the deposition time increases. Starting from a thickness above 1000 μm , the plates are not identified as separate flat objects, but can be considered as a continuous surface (array). Plate turns into an array of individual points and then into a continuous surface. The absence of such plates is clearly visible in the magnified AFM image of a thicker film.

The obtained films have a high transmission capacity in the visible and near-infrared regions of the spectrum of about 70–95%. The high transmittance is suitable for solar cell applications where CdS can be used as a window material in heterojunction solar cells such as CdS/CdTe.

For a film with a thickness of 1215 nm, the transmittance increases with increasing wavelength in the entire range, while for films with a thickness of 420 nm, 515 nm, 520 nm, and 560 nm, there is a rise and fall in the transmittance. Such changes are believed to be caused by the interference of light passing through the thin film and the substrate.

The linear character of the dependences $(\alpha h\nu)^2 = f(h\nu)$ indicates the formation of the absorption edge by direct interband optical transitions.

This study was supported by the Ministry of Education and Science of Ukraine as the project for young scientists "Technology and computer simulation of II generation optimized photovoltaic systems based on compounds II-VI" (0121U108153).

I.V. Vakalyuk – PhD student of Physics and Chemistry of Solids Department;
R.S. Yavorskyi – PhD, Ass.Prof. of Physics and Chemistry of Solids Department;
L.I. Nykyruiy – PhD, Prof. of Physics and Chemistry of Solids Department;
B.P. Naidych – PhD, senior researcher;
Y.S. Yavorskyi – PhD, senior researcher, Head of Labs of Physics and Chemistry of Solids Department.

- [1] A.S. Lahewil, Y. Al-Douri, U. Hashim, N.M. Ahmed, *Structural and optical investigations of cadmium sulfide nanostructures for optoelectronic applications*, Solar Energy, 86(11), 3234 (2012); <https://doi.org/10.1016/j.solener.2012.08.013>.
- [2] N. Amin, K. Sopian, M. Konagai, *Numerical modeling of CdS/CdTe and CdS/CdTe/ZnTe solar cells as a function of CdTe thickness*, Sol. Energy Mater. Sol. Cells, 91(13), 1202 (2007); <https://doi.org/10.1016/j.solmat.2007.04.006>.
- [3] Wisz, G., et al. *TiO₂/Cu₂O heterojunctions for photovoltaic cells application produced by reactive magnetron sputtering*, Materials Today: Proceedings, 35, 552-557, (2021); <https://doi.org/10.1016/j.matpr.2019.10.054>.
- [4] T.L. Chu, S.S. Chu, *Thin film II–VI photovoltaics*, Solid-State Electronics, 38(3), 533 (1995); [https://doi.org/10.1016/0038-1101\(94\)00203-R](https://doi.org/10.1016/0038-1101(94)00203-R).
- [5] O. Vigil, I. Riech, M. Garcia-Rocha, & O. Zelaya-Angel, *Characterization of defect levels in chemically deposited CdS films in the cubic-to-hexagonal phase transition*, Journal of Vacuum Science & Technology A: Vacuum, Surfaces, and Films, 15(4), 2282 (1997); <https://doi.org/10.1116/1.580735>.
- [6] A. Bosio, G. Rosa, N. Romeo, *Past, present and future of the thin film CdTe/CdS solar cells*, Solar Energy, 175, 31 (2018); <https://doi.org/10.1016/j.solener.2018.01.018>.

- [7] N. Akcay, E.P. Zaretskaya, Süleyman Ozelcik, *Development of a CZTS solar cell with CdS buffer layer deposited by RF magnetron sputtering*, Journal of Alloys and Compounds, 772, 782 (2019); <https://doi.org/10.1016/j.jallcom.2018.09.126>.
- [8] N.K. Das, et al., *Effect of substrate temperature on the properties of RF sputtered CdS thin films for solar cell applications*, Results in Physics, 1, 103132 (2020); <https://doi.org/10.1016/j.rinp.2020.103132>.
- [9] G. Balaji, et al., *Investigations on Hot-wall deposited Cadmium Sulphide buffer layer for thin film solar cell*, Materials Letters, 22, 82 (2018); <https://doi.org/10.1016/j.matlet.2018.03.185>.
- [10] A. Abbas, et al. *Structural and chemical evolution of the CdS: O window layer during individual CdTe solar cell processing steps*, Solar Energy, 159, 940 (2018); <https://doi.org/10.1016/j.solener.2017.11.051>.
- [11] M.S. Kale, K.N. Bagad, S.P. Pathak, D.S. Bhavsar, *Growth and Characterizations of CdS Thin Films Grown by Thermal Evaporation Technique*, Int. J. Res. Sci. Innov., 3(7), 84 (2016).
- [12] A.S. Hassaniien, *Studies on dielectric properties, opto-electrical parameters and electronic polarizability of thermally evaporated amorphous Cd₅₀S_{50-x}Se_x thin films*, Journal of Alloys and Compounds, 671, 566 (2016); <https://doi.org/10.1016/j.jallcom.2016.02.126>.
- [13] F. Lisco et al., *The structural properties of CdS deposited by chemical bath deposition and pulsed direct current magnetron sputtering*, Thin solid films, 582, 323 (2015); <https://doi.org/10.1016/j.tsf.2014.11.062>.
- [14] O. Okorie, A.D.A. Buba, A.M. Ramalan, *Optical and dielectric properties of cadmium sulphide thin film grown using chemical bath deposition technique*, IOSR J. Appl. Phys., 9, 82 (2017); <https://doi.org/10.9790/4861-0905018289>.
- [15] A.J. Khimani, S.H. Chaki, T.J. Malek, J.P. Tailor, S.M. Chauhan, M.P. Deshpande, *Cadmium sulphide (CdS) thin films deposited by chemical bath deposition (CBD) and dip coating techniques—a comparative study*, Materials Research Express, 5(3), 036406 (2018); <https://doi.org/10.1088/2053-1591/aab28d>.
- [16] F. Lisco, P.M. Kaminski, A. Abbas, J.W. Bowers, G. Claudio, M. Losurdo, J.M. Walls, *High rate deposition of thin film cadmium sulphide by pulsed direct current magnetron sputtering*, Thin Solid Films, 574, 43 (2015); <https://doi.org/10.1016/j.tsf.2014.11.065>.
- [17] F. Carla, F. Loglio, A. Resta, R. Felici, E. Lastraioli, M. Innocenti, M.L. Foresti, *Electrochemical atomic layer deposition of CdS on Ag single crystals: Effects of substrate orientation on film structure*, The Journal of Physical Chemistry C, 118(12), 6132 (2014); <https://doi.org/10.1021/jp405637g>.
- [18] S. Chaudhuri, J. Bhattacharyya, D. De, A.K. Pal, *Characterization of CdS film prepared by hot wall technique*, Solar energy materials, 10(2), 223 (1984); [https://doi.org/10.1016/0165-1633\(84\)90062-5](https://doi.org/10.1016/0165-1633(84)90062-5).
- [19] Petrus, R., Ilchuk, H., Kashuba, A., Semkiv, I., Zmiiivska, E., Honchar, F., & Lys, R. *Surface-barrier Structures Au/n-CdS: Fabrication and Electrophysical Properties*, Journal of nano- and electronic physics, 11(3), 03020 (2019); [https://doi.org/10.21272/jnep.11\(3\).03020](https://doi.org/10.21272/jnep.11(3).03020).
- [20] S.A. Al Kuhaimi, *Influence of preparation technique on the structural, optical and electrical properties of polycrystalline CdS films*, Vacuum, 51(3), 349 (1998); [https://doi.org/10.1016/S0042-207X\(98\)00112-2](https://doi.org/10.1016/S0042-207X(98)00112-2).
- [21] R. Banerjee, R. Jayakrishnan, P. Ayyub, *Effect of the size-induced structural transformation on the bandgap in CdS nanoparticles*, Journal of Physics: Condensed Matter, 12(50), 10647 (2000); <https://doi.org/10.1088/0953-8984/12/50/325>.
- [22] J.P. Enriquez, X. Mathew, *The effect of annealing on the structure of CdTe films electro-deposited on metallic substrates*, Journal of crystal growth, 259(3), 215 (2003); <https://doi.org/10.1016/j.jcrysgro.2003.07.001>.
- [23] P.K. Kumarasinghe, A. Dissanayake, B.M. Pemasiri, B.S. Dassanayake, *Effect of post deposition heat treatment on microstructure parameters, optical constants and composition of thermally evaporated CdTe thin films*, Materials Science in Semiconductor Processing, 58, 51 (2017); <https://doi.org/10.1016/j.mssp.2016.11.028>.
- [24] J.A. Thornton, D.W. Hoffman, *Stress-related effects in thin films*, Thin solid films, 171(1), 5 (1989); [https://doi.org/10.1016/0040-6090\(89\)90030-8](https://doi.org/10.1016/0040-6090(89)90030-8).
- [25] W. Mahmood, et al. *Optical and electrical studies of CdS thin films with thickness variation*, Optik, 158, 1558 (2018); <https://doi.org/10.1016/j.ijleo.2018.01.045>.
- [26] R.Yu. Petrus, et al., *Optical properties of CdS thin films*, Journal of Applied Spectroscopy, 87(1), 35 (2020); <https://doi.org/10.1007/s10812-020-00959-7>.
- [27] P.P. Sahay, R.K. Nath, S. Tewari, *Optical properties of thermally evaporated CdS thin films*, Crystal Research and Technology, Journal of Experimental and Industrial Crystallography, 42(3), 275 (2007); <https://doi.org/10.1002/crat.200610812>.
- [28] J. Tauc (ed) *Amorphous and liquid semiconductors*. (Springer, Berlin, 2012).
- [29] J.B. Coulter, D.P. Birnie III, *Assessing Tauc plot slope quantification: ZnO thin films as a model system*, Physica status solidi (b), 255(3), 1700393 (2018); <https://doi.org/10.1002/pssb.201700393>.
- [30] S.J. Ikhmayies, R.N. Ahmad-Bitar, *A study of the optical bandgap energy and Urbach tail of spray-deposited CdS: In thin films*, Journal of Materials Research and Technology, 2(3), 221 (2013); <https://doi.org/10.1016/j.jmrt.2013.02.012>.
- [31] P.S. Suryavanshi, C.J. Panchal, *Investigation of Urbach energy of CdS thin films as buffer layer for CIGS thin film solar cell*, Journal of nano- and electronic physics, 10(2), 02012 (2018); <http://essuir.sumdu.edu.ua/handle/123456789/68691>.

- [32] B. Choudhury, A. Choudhury, *Oxygen defect dependent variation of bandgap, Urbach energy and luminescence property of anatase, anatase–rutile mixed phase and of rutile phases of TiO₂ nanoparticles*, Physica E: Low-Dimensional Systems and Nanostructures, 56, 364 (2014); <https://doi.org/10.1016/j.physe.2013.10.014>.
- [33] A.S. Hassanien, A.A. Akl, *Optical characterizations and refractive index dispersion parameters of annealed TiO₂ thin films synthesized by RF-sputtering technique at different flow rates of the reactive oxygen gas*, Physica B: Condensed Matter, 576, 411718 (2020); <https://doi.org/10.1016/j.physb.2019.411718>.
- [34] A. Mukherjee, M.R. Das, A. Banerjee, P. Mitra, *Influence of nickel incorporation in CdS: Structural and electrical studies*, Thin Solid Films, 704, 138005 (2020); <https://doi.org/10.1016/j.tsf.2020.138005>.
- [35] J.C. Manificier et al., *Optical and electrical properties of SnO₂ thin films in relation to their stoichiometric deviation and their crystalline structure*, Thin solid films, 41 (2), 127 (1977); [https://doi.org/10.1016/0040-6090\(77\)90395-9](https://doi.org/10.1016/0040-6090(77)90395-9).
- [36] E. Akbarnejad, M. Ghoranneviss, S. Mohajerzadeh et al., *Optical absorption enhancement of CdTe nanostructures by low-energy nitrogen ion bombardment*. J Phys D Appl Phys. 49, 075301 (2016); <https://doi.org/10.1088/0022-3727/49/7/075301>.
- [37] M.A. Islam, et al., *Comparison of structural and optical properties of CdS thin films grown by CSVT, CBD and sputtering techniques*. Energy Proceedings 33, 203 (2013); <https://doi.org/10.1016/j.egypro.2013.05.059>.
- [38] S. Butt, N.A. Shah, A. Nazir, Z. Ali, A. Maqsood, *Influence of film thickness and In-doping on physical properties of CdS thin films*. Journal of alloys and compounds 587, 582 (2014); <https://doi.org/10.1016/j.jallcom.2013.10.221>.
- [39] Z. Zapukhlyak, et al. *SCAPS simulation of ZnO/CdS/CdTe/CuO heterostructure for photovoltaic application*, Physics and Chemistry of Solid State 21(4), 660-668 (2020); <https://doi.org/10.15330/pcss.21.4.660-668>.
- [40] E. Shaaban, I. Yahia, E. El-Metwally, *Validity of Swanepoel's method for calculating the optical constants of thick films*. Acta physica polonica a 121(3), 628 (2012); <https://doi.org/10.12693/APhysPolA.121.628>.
- [41] R. Swanepoel, *Determination of the thickness and optical constants of amorphous silicon*. Journal of Physics E: Scientific Instruments 16(12), 1214 (1983); <https://doi.org/10.1088/0022-3735/16/12/023>.
- [42] R. Yavorskyi, L. Nykyruy, G. Wisz, P. Potera, S. Adamiak, S. Górny, *Structural and optical properties of cadmium telluride obtained by physical vapor deposition technique*. Applied Nanoscience 9(5), 715 (2019); <https://doi.org/10.1007/s13204-018-0872-z>.
- [43] L. Nykyrui, Y. Saliy, R. Yavorskyi, Y. Yavorskyi, V. Schenderovsky, G. Wisz, & S. Górny, *CdTe vapor phase condensates on (100) Si and glass for solar cells*, In 2017 IEEE 7th International Conference Nanomaterials: Application & Properties (NAP) (pp. 01PCSI26-1), IEEE (2017); <https://doi.org/10.1109/NAP.2017.8190161>.
- [44] R. Yavorskyi, *Features of optical properties of high stable CdTe photovoltaic absorber layer*, Physics and Chemistry of Solid State, 21(2), 243-253 (2020); <https://doi.org/10.15330/pcss.21.2.243-253>.

I.V. Вакалюк, Р.С. Яворський, Л.І. Никируй, Б.П. Найдич, Я.С. Яворський

Морфологія і оптичні властивості тонких плівок CdS, отриманих методом фізичного вакуумного осадження

Vasyl Stefanyk Precarpathian National University, Ivano-Frankivsk, Ukraine, r.yavorskyi@pnu.edu.ua

Досліджено оптичні властивості тонких плівок сульфїду кадмію, отриманих термічним випаровуванням у вакуумі. Використовували стехіометричні склади бінарної сполуки, попередньо синтезовані з високочистих порошоків вихідних компонентів. Плівки різної товщини, нанесені на скляну підкладку, досліджували за допомогою скануючої електронної мікроскопії та визначали коефіцієнт поглинання методом Свейнпола. Встановлено, що зі збільшенням товщини плівки поверхневі утворення зменшуються і при товщині 1 мкм поверхня плівки є суцільною. Визначено, що тонкі плівки сульфїду кадмію мають оптимальні оптичні параметри для використання їх як буферний шар фотоелектричних пристроїв. Усі отримані плівки, крім плівки товщиною 1215 нм, демонструють звичайну інтерференційну картину в спектрах відбиття.

Ключові слова: CdS, PVD, коефіцієнт поглинання, спектри оптичного пропускання, спектри оптичного відбиття, оптична ширина забороненої зони.